A Flux Balancing Strategy for 10-kV SiC-Based Dual-Active-Bridge Converter

Zihan Gao[1], Pengfei Yao[2], Haiguo Li[1], Fred Wang[1,3]
[1]Min H. Kao Department of Electrical Engineering and Computer Science, the University of Tennessee, Knoxville, TN, USA
[2]China Huaneng Group Co., Ltd., Beijing, China
[3]Oak Ridge National Laboratory, Oak Ridge, TN, USA
Email: {zgao15, hli96}prb@vols.utk.edu , yaopf19921210@163.com, fred.wang@utk.edu

2022 IEEE 9th Workshop on Wide Bandgap Power Devices & Applications (WiPDA) | 978-1-6654-8900-3/22/$31.00 ©2022 IEEE | DOI: 10.1109/WiPDA56483.2022.9955288

***Abstract*— The transformer flux unbalance in dual-active-bridge (DAB) converters is a critical issue due to the electrical parameter and modulation mismatch, and load or control transients. Compared to low voltage DAB converters, the unbalance problem in medium voltage DAB converters may cause more severe problem, and become more difficult to deal with, because of the high operating voltage and insulation requirement. In this paper, a flux balancing strategy for a medium voltage (MV) DAB converter is proposed, including the transformer design with ferrite gap, current harmonic-based unbalance detection, as well as the flux balancing control scheme. With the proposed ferrite gap, nonlinear magnetizing current and its modeling are induced. Then, by analyzing the current harmonics, the flux unbalance level can be detected, and hence controlled. Test results have verified the proposed method in a MV DAB converter.**

Keywords—Dual-active-bridge converters; flux balancing; medium voltage

I. INTRODUCTION

Medium voltage (MV) dc/dc converters have increasingly been implemented widely as the dc high power and voltage conversion are needed. The dual-active-bridge (DAB) converters with medium frequency MV transformer are commonly selected as the topology which can transmit power bidirectionally. As the great progress has been made on the wide-bandgap devices, higher and higher MV devices, especially SiC MOSFETs, are available, enabling MV power electronic converters. Along with the technical progress on MV SiC devices and applications, the MV transformers are also under development. Due to the high voltage requirement, the insulation performances of these transformers have to be carefully considered, which also affects the power density and efficiency of the transformers. To improve the performance efforts have been made on analyzing and designing insulation thermal and magnetics.

The MV converters are having higher and higher power densities, leaving less material margin on devices and transformers. However, with converter parameter mismatch, such as channel resistances, switching transition times, or modulation and control transients, volt-second unbalance can be imposed on the transformer impedance, causing dc component in the transformer magnetizing current, and hence biased flux density [1, 2]. The bias in flux density may cause transformer saturation, increase losses, or even damage the MV SiC devices.

To tackle this issue, many approaches on estimation, detection and control have been proposed in the literature, and the methods can be categorized as the methods of modeling or estimating the flux unbalance, the methods of detecting the flux unbalance and methods to compensate the flux unbalance. First, [3-5] introduced the prediction method of potential dc bias in the transformer. Studies also noticed that by using zero-voltage-switching transient [6], the dc bias of the flux can be limited. To detect the flux unbalance, hall-effect and coil-based sensors can be used to measure the magnetizing current, or the core flux density [1]. To improve the sensitivity, other indirect methods can also be adopted, e.g., ferrite "magnetic ear" [7, 8], magnetostriction based sensor [9, 10], or passive impedance-based measurement [11]. For transient flux balancing during load and control transients, the transient modulation schemes have also been well discussed [12, 13]. Nevertheless, due to the high operating voltage and the use of nanocrystalline cores, not all can be implemented in MV DAB converters. New methods with non-contact detection and robust control are desirable for MV DAB converters [14].

In this paper, a second-order harmonic-based indirect flux sensing and balancing scheme for medium-frequency MV transformer and DAB converter is introduced. A magnetic gap is used to create partial saturation and harmonics in the magnetizing current, with which the dc bias of the flux unbalance can be detected and then controlled. The analysis and implementation have been performed for the MV DAB converter. The analysis and tests reveal that the proposed method is feasible in MV DAB converters to prevent transformer saturation caused by flux unbalance.

In Section II, the method of detecting flux unbalance with a non-linear magnetic gap is introduced and validated. In Section III, the control scheme to balance the core flux is then discussed, followed by the test results verifying the scheme in Section IV. Finally, Section V summarizes and concludes the proposed scheme.

This work was supported by the Advanced Manufacturing Office (AMO), United States Department of Energy, under Award no. DE-EE0008410, and made use of the Engineering Research Center Shared Facilities supported by the Engineering Research Center Program of the National Science Foundation and DOE under NSF Award Number EEC-1041877 and the CURENT Industry Partnership Program.

II. HARMONIC-BASED FLUX UNBALANCE DETECTION

A. The Magnetic Gap and Non-Linear Magnetizing Current

As has been discussed in the introduction, several approaches for flux unbalance detection have been introduced. However, for MV transformers, due to the implementation complexity, the current sensing methods is still preferable. Due to the low level of magnetizing current compared to the load current, a strategy must be taken to improve the measurement accuracy. Otherwise, the flux unbalance, which is represented by the dc bias in the magnetizing current will be submerged into the dc offset and sensor noise.

In the utility transformers, discussion and modeling have been made on transformer saturation and magnetizing current harmonics. In [15], current harmonics in the magnetizing current during dc biased flux has been studied. The results of the saturation test of the 50 Hz transformer can also be extended into medium frequency MV transformers. Due to the high operating point, partial saturation may be observed due to the non-linearity of the core, resulting in nonlinear magnetizing current. If the flux DC bias is different, the saturation level within one switching cycle will be different, too. Then, the saturation may be used as the information to sense to extract the flux unbalance level, by which no DC bias measurement will be used for the flux balancing feedback.

As some of the MV transformers tend to have an air gap to prevent saturation due to flux unbalance, one of the ways to introduce non-linearity in the transformer core is to replace the air gap with a magnetic gap. The magnetic gap can be a thin ferrite sheet with a lower saturation flux density, in contrast to the nanocrystalline and amorphous cores. The amorphous material has high permeability and saturating flux density, while the ferrite can have relatively lower permeability and saturation level. If the saturation level of the two materials can be mismatched, a non-linear current curve with a partial saturation can be realized in the magnetizing current.

To verify the introduced non-linearity, a transformer with an amorphous core and ferrite gap has been made and tested as in Fig. 1. The estimated saturation current of the transformer ferrite gap is 2.5 A. The peak-to-peak value of the magnetizing current is around 5 A. In Fig. 1 (a), the flux is symmetrical. The positive and negative half-cycles are also asymmetric, which means different saturation level and the variation of the

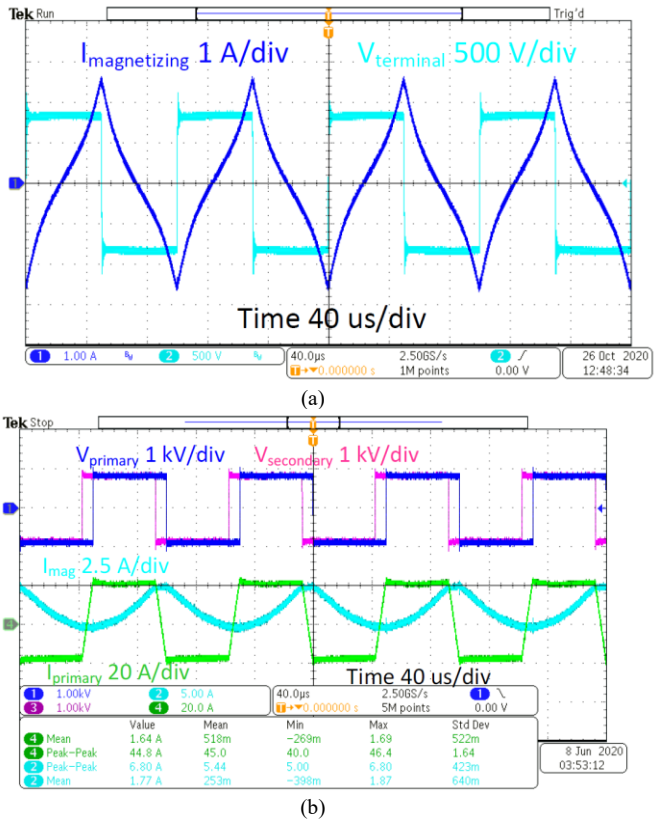

Fig. 1. The current waveform with ferrite gap: (a) balanced flux, (b) unbalanced flux.

magnetizing current, the higher the current, the smaller the inductance, and hence the faster current slope. In Fig. 1 (b), the transformer is working in full load mode, and the DC bias of 1.7 A in magnetizing current is inserted. Similar to the waveforms in Fig. 1 (a), the transformer current is with large distortion, along with the significant DC bias. The peak-to-peak value is 6.8 A. The positive and negative half-cycles are also asymmetric, which means different saturation level and the variation of the magnetizing current, the higher the current, the smaller the inductance.

B. Modeling of the Magnetic Gap in DAB Converters

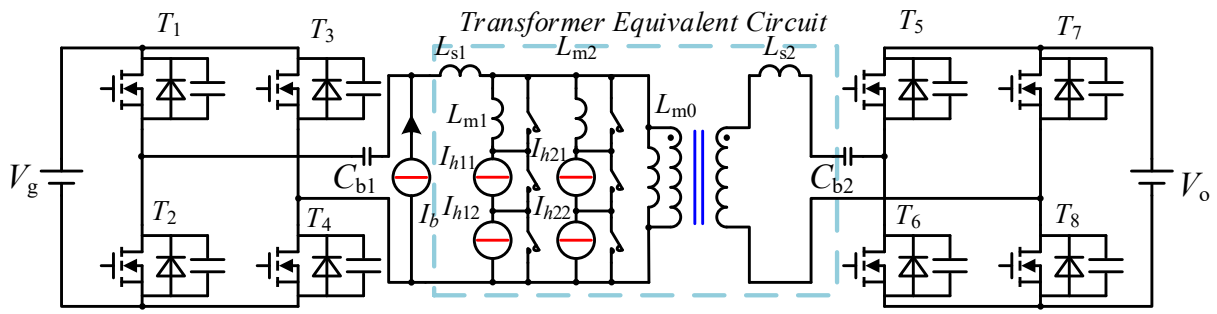

Fig. 2. The model of DAB with ferrite gaped transformer.

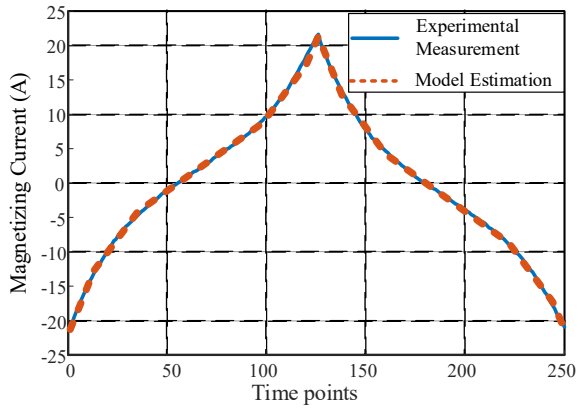

Fig. 3. The curve fitting of transformer magnetizing current with ferrite gap.

To avoid high complexities of analysis, a piecewise linear model can be used to model the proposed transformer with a magnetic gap without considering the detailed permeability change of the combined transformer core. In order to model the partial transformer saturation, an inductive network has to be adopted to have a variant magnetic inductance. The topology of the model is shown in Fig. 2.

In the proposed DAB model, virtual DC blocking capacitors C_{b1}, C_{b2}, are inserted in series with the transformer windings, to avoid DC errors in calculation from the DAB, and paralleled DC source Ib is added to introduce the DC bias current of the magnetizing current. To simplify the analysis, only one side of the transformer has the DC bias. L_{m0} serves as the unsaturated magnetizing inductance, while Lm1 and L_{m2} are the paralleled inductance to mimic the inductance reduction during saturation. Two stages are used to have a smoother transition from the unsaturated state to the saturated state, which will be verified with the curve fitting. Current sources I_{h11}, I_{h12} I_{h21} and I_{h22} with by passing virtual switches are inserted to model the behavior of B-H hysteresis of the saturable ferrite sheets. If the magnetizing inductance of the unsaturated core is L_{nonsat}, ferrite partially saturated L_{pasat}, and ferrite gap fully saturated L_{sat}, the values of L_{m0}, L_{m1} and L_{m2} can be determined as

$$\begin{cases} L_{m0} = L_{unsat} \\ \dfrac{L_{m0}L_{Lm1}}{L_{m0}+L_{m1}} = L_{pasat} \\ \dfrac{L_{m0}L_{m1}L_{m2}}{L_{m0}L_{m1}+L_{m1}L_{m2}+L_{m0}L_{m2}} = L_{sat} \end{cases} \tag{1}$$

As only the steady-state flux unbalance is of interest here, the state-space method has been used to analyze the non-linear behavior of the magnetic gap in the DAB converter. Due to the complexity of the adopted model, the computation of the state space has been performed in the combined platform of Simulink/MATLAB and PLECS, so that the topology can be

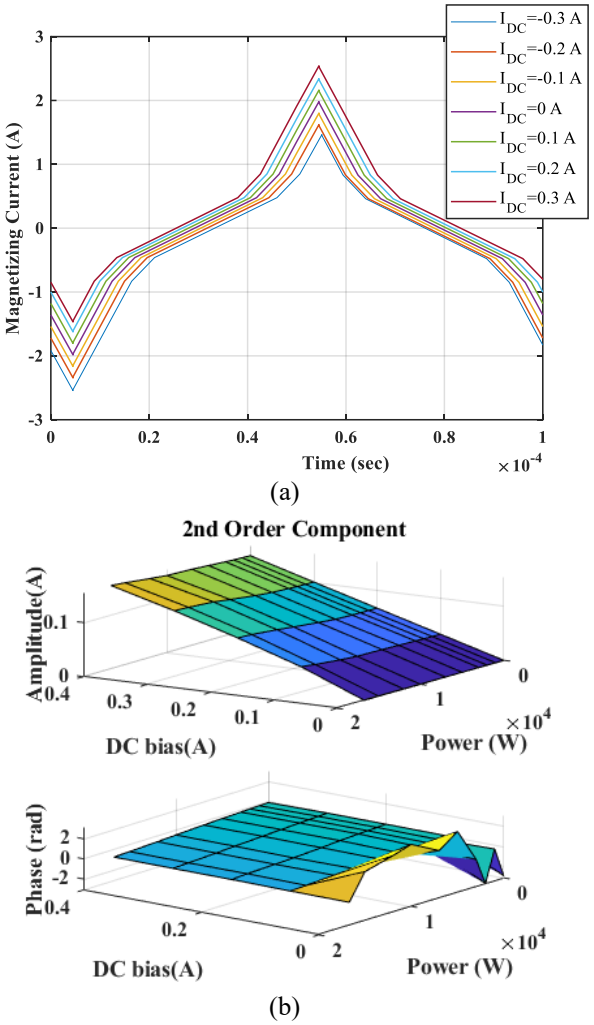

Fig. 4. The modeled transformer current: (a) at different load condition, (b) with different flux unbalance at no load.

easily implemented in Simulink and all the state matrices can be extracted automatically in PLECS. Then, the initial state can be found at the steady state by using the equation of

$$\mathbf{x}_0 = \prod_{i=1}^{k} e^{\tilde{\mathbf{A}}_i t_i} \mathbf{x}_0 \tag{2}$$

Where $\mathbf{x}_0$ stands for the initial vector of state variables in one switching cycle, and $\tilde{\mathbf{A}}_i$ the state matrix at the subinterval i as well as t_i the time duration. The matrix exponential computes the state after one switching interval, in which several intervals model both the saturated and non-saturated transformer states, and finally at the end of the switching cycle the state variables should coincide with the initial condition. Then, with the particle swarm algorithm, both t_i and $\mathbf{x}_0$ can be found with negligible computation error, with the controlled preset saturation level in each branch.

The method has been verified with the open-circuit test of the transformer, and meanwhile the current waveform is also used to curve fitting parameters of the model. In Fig. 3, both test waveform and curve-fitted modeling result have been

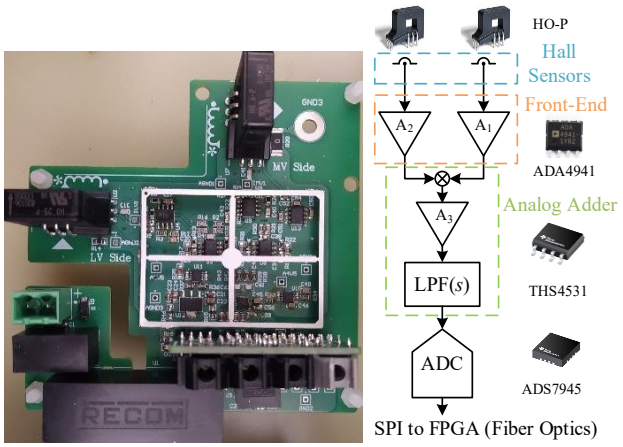

(a) (b)

Fig. 5. (a) photo and (b) diagram of Transformer magnetizing current sensor for MV DAB converter.

shown. To achieve high precision, one core with 4 turns winding has been used to enlarge the current for more accurate measurement. With the test result, the non-saturated inductance is 22 mH, partial transitional saturated 10.46 mH, and ferrite fully saturated 5.85 mH. The threshold of saturation on each branch is 0.44 A and 0.98 A respectively, with a hysteresis of 0.12 A. The curve fitting error is 2.4%.

With the curve-fitted model, the DAB operating waveform can be derived. And the waveform with ferrite gap can be seen in Fig. 4. Then the current harmonic can be extracted from the modeled current at a different level of dc flux unbalance [14].

C. Magnetizing Current Sensing

The proposed scheme of magnetizing current sensor is shown in Fig. 5. To meet the insulation requirement, the two winding currents are sensed separately, with through-hole Hall effect sensors. Then, the two analog signals representing two currents are summed together with the same or different preset gain. The gain is tuned so that the output of the summation circuit should be the magnetizing current, which means the gains of the two scalers should be

$$\frac{A_1}{A_2}\frac{A_{Hall,1}}{A_{Hall,2}} = \frac{N_1}{N_2} \tag{3}$$

where A_1, A_2 are the gains of the scalers, and $A_{Hall,1}$, $A_{Hall,2}$ the Hall sensor gains, N_1, N_2 the winding turns for both sides.

III. Flux Balancing Control

As the detection scheme has been proposed, analyzed, and verified, the corresponding controller can be designed to control both the power conversion of the DAB and also the DC flux of the transformer. The diagram showing both the DAB controller and flux balancing scheme is depicted in Fig. 6. From the control diagram, the DC-link voltage of the output side is sampled, and then a notch filter in the digital controller is used to filter out the second order power harmonic induced

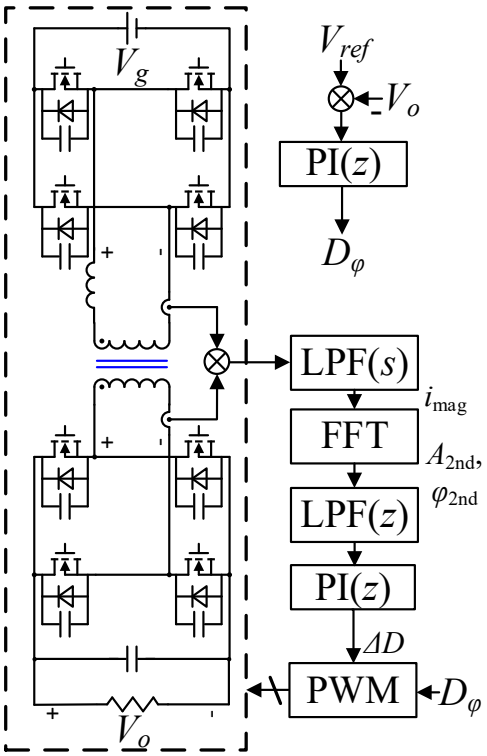

Fig. 6. Control scheme of DAB including flux balancing control.

by the downstream single-phase DC/AC converter. The output voltage is controlled by the PI controller, and then the phase shift reference D is transferred into the pulse-width modulation (PWM) generator.

The sampling frequency of the transformer sensor is of importance, as using a high sampling rate leads to a high cost on board and communication design, while a too low rate may result in poor precision and unstable control response. Since the sampling rate of the flux balancing scheme has to be several times higher than the switching frequency, a reasonable sampling rate is needed. Since only the second order harmonic is needed, 8-point FFT within a single switching can be used. As the switching frequency is 10 kHz, the sampling rate is then 80 kHz, and Nyquist frequency 40 kHz. As high noise from the Hall sensors has been found, digital filters have to be used in the digital controller, after the FFT calculation has been conducted. The signal processing considering noise and polarity of flux unbalance is illustrated in Fig. 7 (a).

The dc offset unbalance and compensation can be injected independently on one side. The duty-cycle compensation ΔD can be added on either the low voltage side, or the high voltage side. In the converters discussed, the compensation is solely added on the duty-cycle of secondary side, or the MV side, as has been found that the MV SiC device has more deviation. The duty cycle compensation is shown in Fig. 7 (b). The corresponding change of the duty-cycle on For each step of the duty cycle change, the volt-second change can be

$$\Delta\lambda = V_{DC} \cdot \Delta t_{PWM} \tag{4}$$

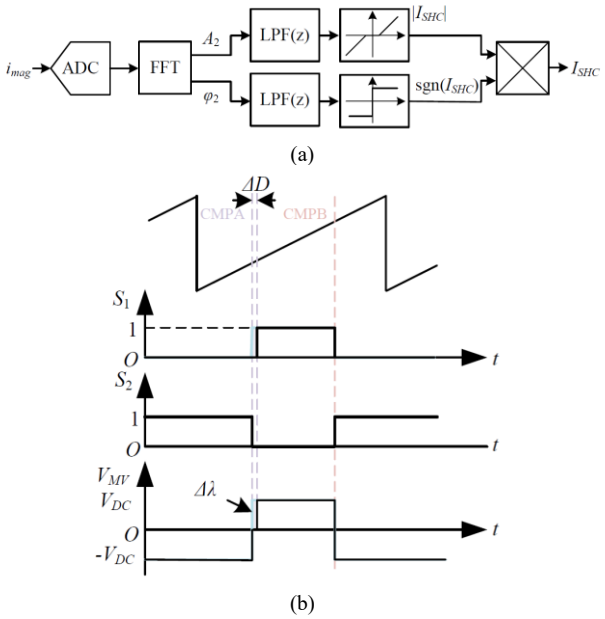

Fig. 7. The diagrams of the (a) second order harmonic signal processing, (b) duty-cycle compensation.

Where $\Delta\lambda$ the change of volt-second product, V_{DC} the DC-link voltage on the compensating side, and Δt_{PWM} the resolution of the PWM modulator.

IV. Test Verification

With the measurement, control, and modulation schemes aforementioned, the complete scheme has been verified in an 850/6700-V DAB converter. The photograph of the MV DAB converter under test is shown in Fig. 8. For the MV DAB converter, the flux balancing detection and control are operating during the test. With some injected volt-second unbalance on MV side, a disturbance can be injected into the magnetizing current, so that the stability of the flux balancing method can be tested.

From Fig. 9, when the volt-second unbalance of 1.5% was injected at the no-load condition, an evident current o set step-up can be found on the magnetizing current, and after around 1.02 second, the envelope of the magnetizing current resumed to the value before the disturbance is added. Unipolar distortion can be found in the magnetizing currents in the lower

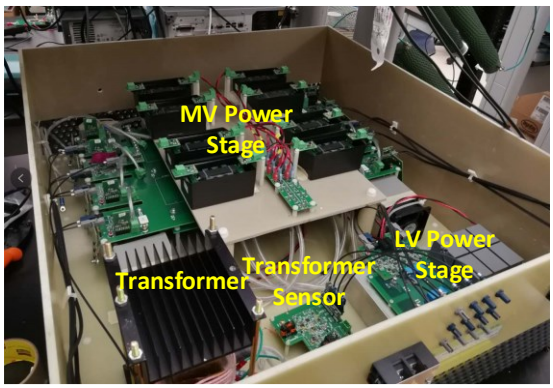

Fig. 8. The photograph of the MV DAB under test.

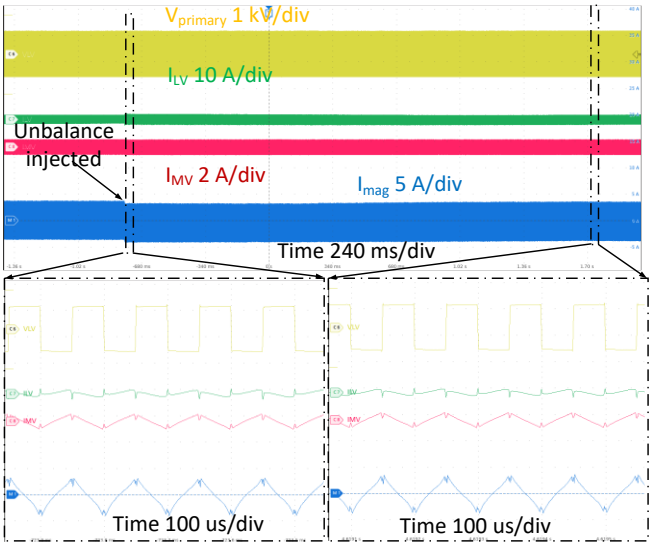

Fig. 9. Test waveform of MV DAB at no load and flux disturbance injection.

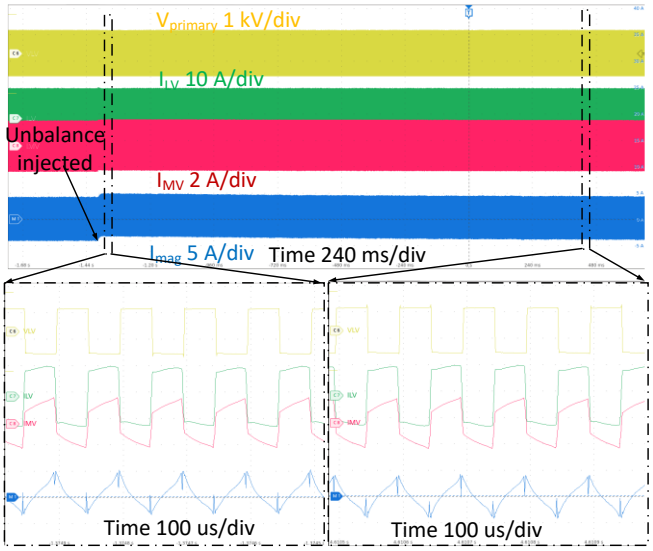

Fig. 10. Test waveform of MV DAB at full load and flux disturbance injection.

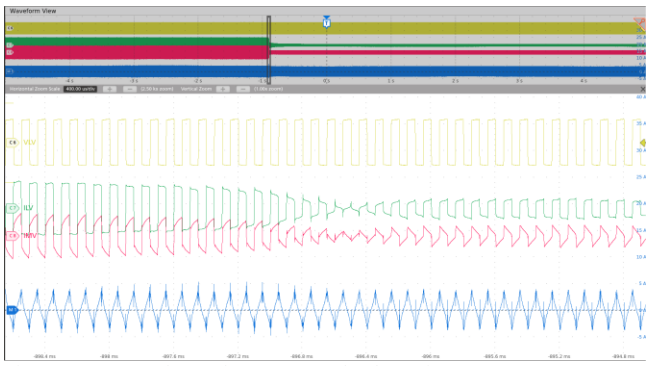

Fig. 11. Test waveform of MV DAB at load transient.

left waveform, the DC bias in the magnetizing current was approximately -1.3 A (reflected on the LV side). After the flux balanced again, in the lower right waveform, the magnetizing

current is more symmetric with control compensation, and the dc component is negligible.

From Fig. 10, at full-load condition, when the volt-second unbalance of 1% was injected, a current offset step-up can be found on the magnetizing current, too, and it took around 0.9 second for the envelope of the magnetizing current to resume the state before the disturbance was injected. The distortion can be found in the magnetizing currents in the lower left zoomed-in curve, the dc bias in the magnetizing current is approximately 2 A. After the flux balanced by the control, in the lower right zoomed-in waveform, the magnetizing current can be balanced, and the DC component is also negligible.

To verify the stability during the load or control transient, a test has been conducted during the load transient from full-load to no-load, shown in Fig. 11. After the full-load from the DAB serving as the load, the current transition can be found on the transformer winding currents, as well as the magnetizing current. The load transition is set after 5 ms.

V. Conclusion

In this paper, a harmonic-based MV transformer flux balancing scheme, considering both the sensing and control, has been introduced and validated through analyses and tests. First, the non-linearity and magnetic gaps of the transformer core have been introduced. By utilizing the non-linearity of ferrite sheet saturation, the flux unbalance can be indirectly measured by detecting the second-order harmonic current. Then, the balancing control has been discussed with considerations on sampling and modulation. Tests have been performed on a MV DAB converter and verified the proposed method. The proposed flux detection and balancing strategy based on current harmonics are feasible with transformers and DAB converters with medium voltage ratings.

Acknowledgment

The authors want to thank Powerex and Southern Company for providing help on this work.

References

[1] P. Yao, X. Jiang, P. Xue, S. Ji, and F. Wang, "Flux Balancing Control of Ungapped Nanocrystalline Core-Based Transformer in Dual Active Bridge Converters," *IEEE Transactions on Power Electronics,* vol. 35, no. 11, pp. 11463-11474, 2020.

[2] P. Yao, X. Jiang, P. Xue, S. Li, S. Lu, and F. Wang, "Design Optimization of Medium Frequency Transformer for DAB Converters with DC Bias Capacity," *IEEE Journal of Emerging and Selected Topics in Power Electronics,* pp. 1-1, 2020.

[3] D. Yuan, J. Yang, Y. Liu, Y. Jia, R. Liu, and Z. Song, "A Prediction Method of DC Bias for DC-DC Dual-active-bridge Converter with MOSFETs," in *2019 14th IEEE Conference on Industrial Electronics and Applications (ICIEA)*, 19-21 June 2019, pp. 1228-1232.

[4] L. Shu, W. Chen, Z. Lin, D. Ma, X. He, and W. A. Syed, "DC Bias Study for DC-DC Dual-Active-Bridge Converter," in *2018 IEEE 4th Southern Power Electronics Conference (SPEC)*, 10-13 Dec. 2018, pp. 1-5.

[5] L. Shu, W. Chen, and Z. Song, "Prediction method of DC bias in DC-DC dual-active-bridge converter," *CPSS Transactions on Power Electronics and Applications,* vol. 4, no. 2, pp. 152-162, 2019.

[6] D. Costinett, D. Seltzer, D. Maksimovic, and R. Zane, "Inherent volt-second balancing of magnetic devices in zero-voltage switched power converters," in *2013 Twenty-Eighth Annual IEEE Applied Power Electronics Conference and Exposition (APEC)*, 17-21 March 2013 2013, pp. 9-15.

[7] G. Ortiz, L. Fässler, J. W. Kolar, and O. Apeldoorn, "Application of the magnetic ear for flux balancing of a 160kW/20kHz DC-DC converter transformer," in *2013 Twenty-Eighth Annual IEEE Applied Power Electronics Conference and Exposition (APEC)*, 17-21 March 2013, pp. 2118-2124.

[8] G. Ortiz, L. Fässler, J. W. Kolar, and O. Apeldoorn, "Flux Balancing of Isolation Transformers and Application of "The Magnetic Ear" for Closed-Loop Volt–Second Compensation," *IEEE Transactions on Power Electronics,* vol. 29, no. 8, pp. 4078-4090, 2014.

[9] L. Schrittwieser, M. Mauerer, D. Bortis, G. Ortiz, and J. W. Kolar, "Novel principle for flux sensing in the application of a DC + AC current sensor," in *2014 International Power Electronics Conference (IPEC-Hiroshima 2014 - ECCE ASIA)*, 18-21 May 2014 2014, pp. 1291-1298.

[10] L. Schrittwieser, M. Mauerer, D. Bortis, G. Ortiz, and J. W. Kolar, "Novel Principle for Flux Sensing in the Application of a DC + AC Current Sensor," *IEEE Transactions on Industry Applications,* vol. 51, no. 5, pp. 4100-4110, 2015.

[11] L. Zhu, H. Bai, A. Brown, and M. McAmmond, "Design a 400 V–12 V 6 kW Bidirectional Auxiliary Power Module for Electric or Autonomous Vehicles With Fast Precharge Dynamics and Zero DC-Bias Current," *IEEE Transactions on Power Electronics,* vol. 36, no. 5, pp. 5323-5335, 2021.

[12] B. Zhao, Q. Song, W. Liu, and Y. Zhao, "Transient DC Bias and Current Impact Effects of High-Frequency-Isolated Bidirectional DC–DC Converter in Practice," *IEEE Transactions on Power Electronics,* vol. 31, no. 4, pp. 3203-3216, 2016.

[13] M. Stojadinović, E. Kalkounis, F. Jauch, and J. Biela, "Generalized PWM generator with transformer flux balancing for dual active bridge converter," in *2017 19th European Conference on Power Electronics and Applications (EPE'17 ECCE Europe)*, 11-14 Sept. 2017 2017, pp. P.1-P.10.

[14] Z. Gao *et al.*, "A Transformer Flux Balancing Scheme Based on Magnetizing Current Harmonic in Dual-Active-Bridge Converters," in *2021 IEEE Applied Power Electronics Conference and Exposition (APEC)*, 14-17 June 2021 2021, pp. 1894-1899.

[15] Z. Xiaoxin, L. Huiqi, L. Yang, Z. Xiaojun, and C. Zhiguang, "Analysis of the DC bias phenomenon by the harmonic balance method based on the electromagnetic coupling model," in *2013 IEEE INTERNATIONAL CONFERENCE ON MICROWAVE TECHNOLOGY & COMPUTATIONAL ELECTROMAGNETICS*, 25-28 Aug. 2013, pp. 387-390.